

Proton–neutron pair correlations in neutron-rich nuclei

Kenichi Yoshida^{1,2,3,*}

¹*Research Center for Nuclear Physics, Osaka University, Ibaraki, Osaka 567-0047 Japan*

²*RIKEN Nishina Center for Accelerator-Based Science, Wako, Saitama 351-0198, Japan*

³*Center for Computational Sciences, University of Tsukuba, Tsukuba, Ibaraki 305-8577, Japan*

(Dated: November 22, 2024)

Background: Nuclear pairing is a well-established many-body correlation, particularly among like particles in a spin-singlet state. However, the strength of spin-triplet proton–neutron (pn) pairing in nuclei has remained a long-standing and unresolved issue.

Purpose: The relative strength of spin-triplet pn pairing compared to spin-singlet one is investigated by introducing and analyzing the polarizability of the response to pn pair transfers.

Method: The nuclear energy-density functional method is employed. The ground state of the target nucleus is described using the Hartree–Fock–Bogoliubov approximation, which accounts for the conventional superfluidity of like-particle pairs. The response to pn pair transfers is then analyzed using the pn quasiparticle random-phase approximation.

Results: The spin-singlet pn-pair correlation is strongest at $N = Z$ and decreases monotonically with the increasing number of excess neutrons, whereas the spin-triplet pn-pair correlation is shown to depend non-monotonically on the neutron number and can be enhanced in cases where the pn-pair transfers involving the $\pi j_> \otimes \nu j_<$ configuration occur at low energy.

Conclusions: The shell effect, which uniquely appears in spin-triplet pn-pair correlation, serves as a key indicator of the strength of pn-pair correlations.

I. INTRODUCTION

Pairing is a correlation occurring universally in assemblages made of interacting many particles, ranging from quark and nuclear to electron many-body systems. In infinite systems, the correlation is quantified by the introduction of an order parameter, specifically the pairing gap, which arises from condensation. When the correlation is sufficiently strong, fluctuations become significant, leading to a phase transition and the emergence of condensation.

An analogy to superconductivity has been applied to finite nuclei by employing the Bardeen–Cooper–Schrieffer (BCS) theory [1] to the nuclear Hamiltonian [2, 3]. Closed-shell nuclei are in a normal phase, where the gap function vanishes, while most nuclei exhibit a superconducting/superfluid phase at low energy. A non-vanishing pairing gap in the spin-singlet channel plays a central role in various low-energy nuclear phenomena, including the ground-state spin, staggering in the systematics of binding energies, low-lying quadrupole collective dynamics, rotational moments of inertia, and spontaneous fission half-lives [4]. A notable feature unique to finite systems is that pairing can be probed in response to a field changing the number of particles; the pair correlation leads to an enhanced two-nucleon transfer reaction [5].

Heavy proton-rich nuclei along the $N = Z$ line have received a great deal of attention with the advancement of experimental techniques in rare-isotope beams for nuclear physics. Of particular interest is the possible ap-

pearance of exotic phenomena, attributed to the coherent shell effects of both protons and neutrons. Specifically, the spin-triplet proton–neutron (pn) pair correlation is expected to be visible, as the spatial overlap between the proton and neutron single-particle wave functions would be large to form a Cooper pair of a proton and a neutron—a phenomenon initially predicted in light $N = Z$ nuclei [6]. Moreover, the possible coexistence of the spin-singlet pn-pair condensation with the spin-triplet one is predicted [7, 8].

Spin-orbit splitting is crucial in determining whether spin-triplet or spin-singlet pair correlation is stronger in medium-heavy nuclei [9]. If a nucleus is large enough that the surface spin-orbit potential can be neglected, the spin-triplet pn-pair superfluid appears in the ground state [10], as is expected in symmetric nuclear matter [11–14]. However, in reality, spin-orbit splitting suppresses spin-triplet pn-pair correlation in finite nuclei. Consequently, despite numerous attempts, the experimental evidence for spin-triplet pair condensation remains a topic of ongoing debate [15].

The present work further investigates the role of spin-orbit splitting to garner a deeper insight into the pn-pair correlations in medium-heavy nuclei. Previous studies have focused primarily on $N \approx Z$ nuclei, where the correlation between a proton and a neutron is the strongest. However, as demonstrated in Ref. [8], stepping away from the $N = Z$ line can also reveal unexpected and novel findings. In this study, I explore the pn-pair correlations across a wide mass region from calcium to tin isotopes, extending from the $N = Z$ line to the neutron-rich side. To systematically study the pn-pair correlations, I employ the notion of the fluctuation of order parameters.

The paper is organized as follows. In Sec. II, I re-

* E-mail: kyoshida@rcnp.osaka-u.ac.jp

hash the static polarizability/susceptibility in response to an external field and then extend it to the case for the response to pn-pair transfers. A numerical method I employ is briefly summarized in Sec. II C. In Sec. III, I show the results and discuss the roles of excess neutrons on the pn-pair polarizabilities. Section IV summarizes the paper.

II. THEORETICAL FRAMEWORK

A. Static polarizability

To explore the collectivity, one may perform the constrained Hartree–Fock–Bogoliubov (HFB) calculations in the presence of an external field $\lambda\hat{F}$ relevant to the collective mode, i.e. one solves

$$\delta \langle \phi(\lambda) | \hat{H} - \lambda\hat{F} | \phi(\lambda) \rangle = 0, \quad (1)$$

where \hat{H} is the Hamiltonian and $|\phi\rangle$ the HFB state vector. The static polarizability α is defined by the change of the expectation value of \hat{F} [3]:

$$\langle \phi(\lambda) | \hat{F} | \phi(\lambda) \rangle = \langle \phi_0 | \hat{F} | \phi_0 \rangle + \lambda\alpha \quad (2)$$

and the change in energy is given by

$$\langle \phi(\lambda) | \hat{H} | \phi(\lambda) \rangle = \langle \phi_0 | \hat{H} | \phi_0 \rangle + \frac{1}{2}\lambda^2\alpha, \quad (3)$$

where $|\phi_0\rangle = |\phi(0)\rangle$ is the solution of the HFB equation. One then evaluates the static polarizability, the radius of curvature of the potential energy surface at the HFB equilibrium, as

$$\alpha = \frac{d^2}{d\lambda^2} \langle \phi(\lambda) | \hat{H} | \phi(\lambda) \rangle |_{\lambda=0}. \quad (4)$$

Alternatively, one can compute the response functions $R_F(\omega)$ of the system to the external field \hat{F} in the random-phase approximation (RPA):

$$R_F(\omega) = \sum_n \left(\frac{|\langle n | \hat{F} | 0 \rangle|^2}{\omega - \omega_n + i\eta} - \frac{|\langle 0 | \hat{F} | n \rangle|^2}{\omega + \omega_n + i\eta} \right), \quad (5)$$

where $|n\rangle$ and ω_n denote the RPA eigenstates and eigenenergies. If one is interested in the static polarizability, it is sufficient to calculate the inversely-energy weighted sum (IEWS) of the strength distribution:

$$\alpha = -R_F(0) = 2m_{-1}(F), \quad (6)$$

with $m_k(F)$ being the k -th moment of the strength distribution. This is nothing but the dielectric theorem [16].

It is noted that the IEWS and the static polarizability have been discussed intensively for the case of the $E1$ strength function, i.e. the electric dipole excitation in nuclei, as a probe of neutron skin and nuclear matter properties [17–19]. Quite recently, the pair collectivity has been studied in terms of the pair polarizability [20].

B. Polarizability for proton–neutron pairing

The pair field with spin S and isospin T is defined as

$$\hat{P}_{ST}(\mathbf{r}) := \frac{1}{2\sqrt{2}} \sum_{ss'} \sum_{tt'} \hat{\psi}(\mathbf{r}\tilde{s}'\tilde{t}') \hat{\psi}(\mathbf{r}st) S_{S\mu_\sigma, s's} T_{T\mu_\tau, t't} \quad (7)$$

with the nucleon field operator $\hat{\psi}(\mathbf{r}st)$, and $\hat{\psi}(\mathbf{r}\tilde{s}\tilde{t}) := (-2s)(-2t)\hat{\psi}(\mathbf{r}-s-t)$. The spin and isospin operators are defined as

$$S_{00} = 1, \quad S_{1\mu_\sigma} = \sigma_{\mu_\sigma}, \quad (8)$$

$$T_{00} = 1, \quad T_{1\mu_\tau} = \tau_{\mu_\tau}. \quad (9)$$

Here, σ_{μ_σ} and τ_{μ_τ} are the spherical components of spin and isospin Pauli matrices, respectively; $s = \pm 1/2$ stands for the z -component of spin; $t = \pm 1/2$ stands for neutron and proton. The factor of $1/\sqrt{2}$ is put here so that the two-neutron pair field ($\mu_\tau = 1$) coincides with the pair field operator given in Ref. [20]. Note that it is convenient to introduce the factor of $1/\sqrt{2}$ when investigating the isovector modes of excitation with $T_z = \pm 1$ and $T_z = 0$ simultaneously [21].

One can expect the pn-pair correlations to be probed by the response of the pn-pair transfers [22, 23]. I then introduce an $L = 0$ pn-pair addition operator

$$\hat{P}_{ST}^{\text{ad}} := \int d\mathbf{r} Y_{00}(\hat{r}) f(r) \hat{P}_{ST}^\dagger(\mathbf{r}) \quad (10)$$

and an $L = 0$ pn-pair removal operator

$$\hat{P}_{ST}^{\text{rm}} := \int d\mathbf{r} Y_{00}(\hat{r}) f(r) \hat{P}_{ST}(\mathbf{r}), \quad (11)$$

with $\mu_\tau = 0$ for $T = 1$. These operators bring about a transition, which changes the particle number $\Delta N = \pm 2$ with $\Delta T_z = 0$. As in the study of a two-neutron transfer [20], I introduced a form factor $f(r)$, which is effective in a spatial region where the nucleon density is finite, but vanishes far outside the nucleus, as I am interested in a process where a pn pair is added to or removed from a nucleus. Specifically, I choose a Woods–Saxon function

$$f(r) = \frac{1}{1 + e^{(r-R)/a}} \quad (12)$$

with $R = 1.27 \times A^{1/3}$ fm and $a = 0.67$ fm, but as shown later the main conclusion does not depend on a detailed form of $f(r)$. Here, Y_{00} is a spherical harmonics with rank 0 and both \hat{P}^{ad} and \hat{P}^{rm} carry the angular and parity quantum numbers 0^+ . I describe the pn-pair vibration with spin–parity $J^\pi = 0^+$ and 1^+ for $(S, T) = (0, 1)$ and $(1, 0)$, respectively.

I investigate the static polarizability as a measure of the pn pairing. One may consider the polarizability for the hermitian operators $\hat{P}^{\text{ad}} + \hat{P}^{\text{rm}}$ and $i(\hat{P}^{\text{ad}} - \hat{P}^{\text{rm}})$.

They indeed correspond to the operators for the amplitude and phase modes, respectively [20]. Therefore, the order parameter of the pn pairing is $\langle \phi_0 | \hat{P}_{ST}^A | \phi_0 \rangle$ with $\hat{P}_{ST}^A = \hat{P}_{ST}^{\text{ad}} + \hat{P}_{ST}^{\text{rm}}$. The polarizability appropriate for the pair collectivity is then evaluated as

$$\alpha_{ST} = 2 \sum_n \frac{|\langle n | \hat{P}_{ST}^A | 0 \rangle|^2}{\omega_n}, \quad (13)$$

which is an extension of the two-neutron pair polarizability in Ref. [20] to the case for the pn pair.

I assume in the present investigation that the condensation of the pn pairs ($T_z = 0$) does not occur in the ground state: $\langle \phi_0 | \hat{P}_{ST}^{\text{ad}} | \phi_0 \rangle = \langle \phi_0 | \hat{P}_{ST}^{\text{rm}} | \phi_0 \rangle = 0$ for both $(S, T) = (0, 1)$ and $(1, 0)$. In this case, the pn-pair polarizability reads

$$\alpha_{ST} = 2 \sum_n \left(\frac{|\langle n | \hat{P}_{ST}^{\text{ad}} | 0 \rangle|^2}{\omega_n} + \frac{|\langle n | \hat{P}_{ST}^{\text{rm}} | 0 \rangle|^2}{\omega_n} \right). \quad (14)$$

If the system tends to break the symmetry, one sees the polarizability gets diverged, or one obtains the imaginary solution of the RPA equation.

The static polarizability depends on the form of an operator. The reaction mechanism also enters into the form factor. In envisioning the pn-transfer reactions, such as $(p, {}^3\text{He})$ and $({}^3\text{He}, p)$, in which the isoscalar (IS) and isovector (IV) transfers are both allowed, what is proposed here is the ratio of the polarizabilities of the pn pair with $(S, T) = (0, 1)$ and $(1, 0)$:

$$\mathcal{R}_{01} := 3 \frac{\alpha_{01}}{\alpha_{10}}. \quad (15)$$

A factor of three is introduced here to cancel out the spin degeneracy $2S + 1$. When the \mathcal{R}_{01} value is greater than unity, the $S = 0, T = 1$ pn pairing is dominant over the $S = 1, T = 0$ pn pairing. As in the ratio of the pn-transfer cross sections from the ground state of an even-even nucleus to the 0_1^+ and 1_1^+ states in an odd-odd nucleus, one can expect systematic uncertainties and, to some extent, kinematic conditions of the reaction cancel out [24].

C. Numerical Calculations

As a numerical approach for the present investigation, I employ the nuclear energy-density functional (EDF) method. Since the details can be found in Ref. [25], here I briefly recapitulate the basic equations relevant to the present study.

The ground state of a mother (target) nucleus is described by solving the HFB or Kohn–Sham–Bogoliubov

(KSB) equation [26]:

$$\sum_{s'} \begin{bmatrix} h_{ss'}^q(\mathbf{r}) - \lambda^q \delta_{ss'} & \tilde{h}_{ss'}^q(\mathbf{r}) \\ \tilde{h}_{ss'}^q(\mathbf{r}) & -h_{ss'}^q(\mathbf{r}) + \lambda^q \delta_{ss'} \end{bmatrix} \begin{bmatrix} \varphi_{1,\alpha}^q(\mathbf{r}s') \\ \varphi_{2,\alpha}^q(\mathbf{r}s') \end{bmatrix} = E_\alpha \begin{bmatrix} \varphi_{1,\alpha}^q(\mathbf{r}s) \\ \varphi_{2,\alpha}^q(\mathbf{r}s) \end{bmatrix}, \quad (16)$$

where the single-particle and pair Hamiltonians, $h_{ss'}^q(\mathbf{r})$ and $\tilde{h}_{ss'}^q(\mathbf{r})$, are given by the functional derivative of the EDF with respect to the particle density and the pair density, respectively. An explicit expression of the Hamiltonians is found in the Appendix of Ref. [27]. The superscript q denotes ν (neutron, $t = 1/2$) or π (proton, $t = -1/2$). The average particle number is fixed at the desired value by adjusting the chemical potential λ^q . When the system is in the normal phase, the chemical potential is defined by averaging the highest occupied single-particle energy and the lowest unoccupied single-particle energy. Assuming the system is axially symmetric, the KSB equation (16) is block diagonalized according to the quantum number Ω , the z -component of the total angular momentum. As mentioned in the above, I further assumed that the condensation of the pn pairs ($T_z = 0$) does not occur but that of the like-particle pairs ($T_z = \pm 1$) can happen in the ground state.

I solve the KSB equation in the coordinate space using cylindrical coordinates $\mathbf{r} = (\varrho, z, \phi)$. Since I assume further the reflection symmetry, only the region of $z \geq 0$ is considered. I use a two-dimensional lattice mesh with $\varrho_i = (i - 1/2)h$, $z_j = (j - 1)h$ ($i, j = 1, 2, \dots$) with a mesh size of $h = 0.6$ fm and 25 points for each direction. The qp states are truncated according to the qp energy cutoff at 60 MeV, and the qp states up to the magnetic quantum number $\Omega = 31/2$ with positive and negative parities are included.

The excited states in a neighboring odd-odd nucleus $|n\rangle$ are described as one-phonon excitations built on the ground state $|0\rangle$ of the even-even mother nucleus as

$$|n\rangle = \hat{\Gamma}_n^\dagger |0\rangle, \quad (17)$$

$$\hat{\Gamma}_n^\dagger = \sum_{\alpha\beta} \left\{ X_{\alpha\beta}^n \hat{a}_\alpha^\dagger \hat{a}_\beta^\dagger - Y_{\alpha\beta}^n \hat{a}_\beta \hat{a}_{\bar{\alpha}} \right\}, \quad (18)$$

where \hat{a}^\dagger and \hat{a} are the quasiparticle (qp) creation and annihilation operators that are defined in terms of the solutions of the KSB equation (16) with the Bogoliubov transformation. The phonon states, the amplitudes X^n, Y^n and the vibrational frequency ω_n , are obtained in the quasiparticle-RPA (QRPA): the linearized time-dependent density-functional theory for superfluid systems [28]. The EDF gives the residual interactions entering into the QRPA equation. For the axially symmetric nuclei, the QRPA equation is block diagonalized according to the quantum number $K = \Omega_\alpha + \Omega_\beta$.

In solving the QRPA equation, I introduce the truncation for the two-quasiparticle (2qp) configurations, in

terms of the 2qp-energy as 60 MeV. The calculated energy and transition strength of the low-lying and giant resonance states are almost converged with respect to the mesh size, the box size, and the energy cutoff [29], and are compatible with the results obtained in different methodology [30, 31].

For the normal (particle-hole) part of the EDF \mathcal{E}_{ph} , I employ the Skyrme-type SGII functional [32]. For the pairing energy $\mathcal{E}_{\text{pair}}$, I adopt the one in Ref. [33] that depends on both the IS and IV densities, in addition to the pair density, with the parameters given in Table III of Ref. [33]. The same pair interaction is employed for the dynamical pairing for the $S = 0$ and $S = 1$ pn pairs in the QRPA calculation, while the linear term in the IV density is dropped. I multiply a factor f to the pairing EDF for $S = 1$: $\mathcal{E}_{\text{pair}}^{S=1} = f \times \mathcal{E}_{\text{pair}}^{S=0}$ to study the roles of the dynamic spin-triplet pairing. Note that the QRPA calculations including the dynamic spin-triplet pairing with more or less the same strength as the spin-singlet pairing ($f \sim 1$) describe well the characteristic low-lying Gamow-Teller strength distributions in the light $N \simeq Z$ nuclei [34–36], and the β -decay half-lives of neutron-rich Ni isotopes [37].

III. RESULTS AND DISCUSSION

A. Ca isotopes

Figure 1 shows the calculated strength functions for the pair-addition and removal processes in ^{40}Ca . A possible appearance of the collective states in the pn-pair transfer from ^{40}Ca was discussed in Ref. [38]. However, only the lowest 1^+ state in the odd-odd neighboring nuclei, ^{42}Sc and ^{38}K , was investigated as a collective state of the $S = 1$ pn pairing.

As is observed in the figure, not only the lowest state but also the higher-lying states acquire appreciable strengths for both the $S = 0$ and $S = 1$ pn-pair transfers. The occurrence of the higher-lying states is due to the shell structure: The second 0^+ state seen in the pn-pair addition is mainly generated by the $\nu p_{3/2} \otimes \nu p_{3/2}$ configuration with an admixture of $\nu p_{1/2} \otimes \nu p_{1/2}$; while the second 1^+ state is constructed by the $\nu p_{3/2} \otimes \nu p_{1/2}$ and $\nu p_{1/2} \otimes \nu p_{3/2}$ configurations additionally. One can see there are several states even above 20 MeV. These states may also be regarded as pair-vibrational states as the excitation energies are lowered and the pair-transfer strengths are enhanced by the RPA correlation, as compared with the unperturbed strength functions depicted in Figs. 1(b) and 1(d). Although high-lying pair vibration is often called the giant pair vibration [39–42], I adopt in the present paper, following Ref. [20], the more inclusive term “high-lying pair vibrations” for these peaks since the strength distribution does not form a single resonance peak but rather multiple peaks in a wide energy interval.

The primal motivation to introduce the pair polariz-

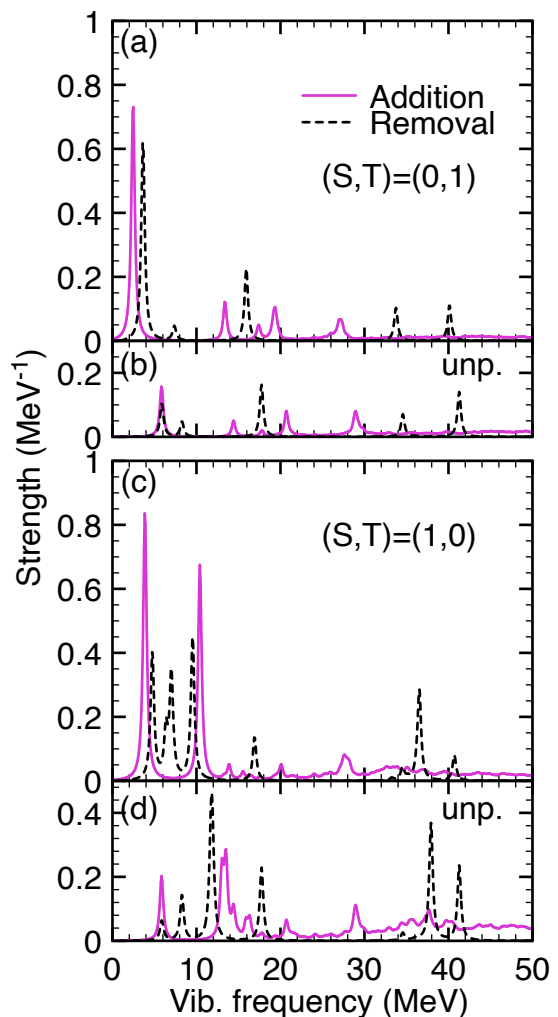


FIG. 1. Calculated pair addition and removal strengths in ^{40}Ca smeared by a Lorentzian function with a width parameter of 0.5 MeV. (a): $S = 0$ pn-pair strengths. (b): Unperturbed $S = 0$ pn-pair strengths. (c): $S = 1$ pn-pair strengths with $f = 1.0$. (d): Unperturbed $S = 1$ pn-pair strengths.

ability in the present study is to relate the pair vibrations distributed in a broad energy region with the macroscopic picture as an amplitude oscillation of the order parameter. The polarizability is defined by the inversely-energy-weight sum of the strength functions, as given in Eq. (14). The low-lying pair vibrational states make a substantial contribution to polarizability. The high-lying pair vibrations can additionally play a role. Figure 2 shows a running sum in Eq. (14) up to E_{max} , where the upper bound E_{max} is varied for ^{40}Ca with $f = 1.0$. The low-lying states below 15 MeV are dominant for the polarizability, and more than 90% of the polarizability is given by the states up to 25 MeV. This is similar to the finding in Ref. [20].

Figure 3(a) shows the polarizabilities for pn-pair transfers with $(S, T) = (0, 1)$ and $(1, 0)$. The $S = 1$ pn-pair polarizability has a peak at $N = Z$ and drops with an

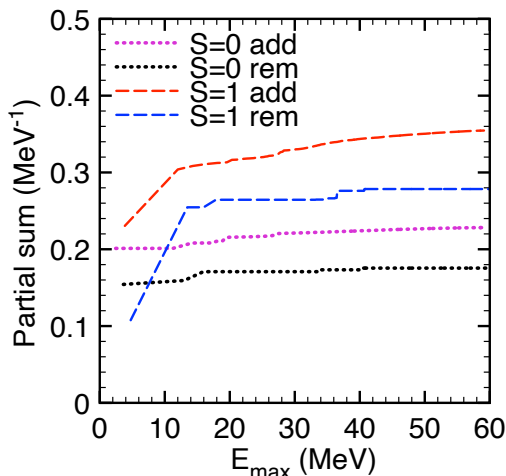


FIG. 2. The inversely-energy-weighted sum of the pn-pair addition and removal strength functions for ^{40}Ca , as a function of the maximum energy E_{max} of the sum: $\omega_n < E_{\text{max}}$.

increase in the neutron number. This is what one would expect: the pn-pair correlation is strongest at $N = Z$ and gets weaker with the neutron excess. Without the $S = 1$ pn-pair interaction ($f = 0$), the $S = 1$ pn-pair polarizability keeps constant at a low value. When considering the pn-pair interaction in the $S = 1$ channel with $f > 0$, the polarizability shows maximal at $N = Z$ and decreases with increasing the neutron number. However, one sees the persistence around $N = 30$. Beyond ^{48}Ca , the $\nu f_{5/2}$ orbital is located near the Fermi level, and then the $S = 1$ pairs of the $\pi f_{7/2} \otimes \nu f_{5/2}$ configuration are created with low energy.

It would not be easy to obtain the absolute values of the pair polarizability since the reaction condition is involved. Instead, the isotopic dependence of the pair polarizability of $S = 0$ and $S = 1$ provides us with information on pair collectivity, as the shell effect uniquely appears in the $S = 1$ pn-pair transfer. Alternatively, by taking the ratio of the pair polarizabilities of $S = 0$ and $S = 1$, one can gain insight into the pairing collectivity. The ratio \mathcal{R}_{01} for the Ca isotopes are shown in Fig. 3(b). Without the pn-pair interaction in the $S = 1$ channel, it is evident that the $S = 0$ pairing is dominant in $N \approx Z$ isotopes: the \mathcal{R}_{01} value is far above the unity. Even with a reasonable strength ($f = 1.0$) of the $S = 1$ pn pair interaction, the $S = 0$ pairing is stronger than the $S = 1$ pairing around $N = Z$. However, the $S = 0$ and $S = 1$ pair correlations vie in collectivity around ^{50}Ca .

In the calculation with $f = 1.3$, the lowest 1^+ state is lower than the 0^+ state by 0.6 (0.2) MeV for the pn-pair addition (removal) transfer, and the transition strength to the 1^+ state is strongly enhanced for ^{40}Ca . It seems that the system is close to the critical point of the $S = 1$ pn-pair condensation; the \mathcal{R}_{01} value is about 0.5. In reality, however, the $S = 1$ pn-pairing is not so strong because the 1^+ state is higher in energy than the 0^+ state in ^{42}Sc and ^{38}K .

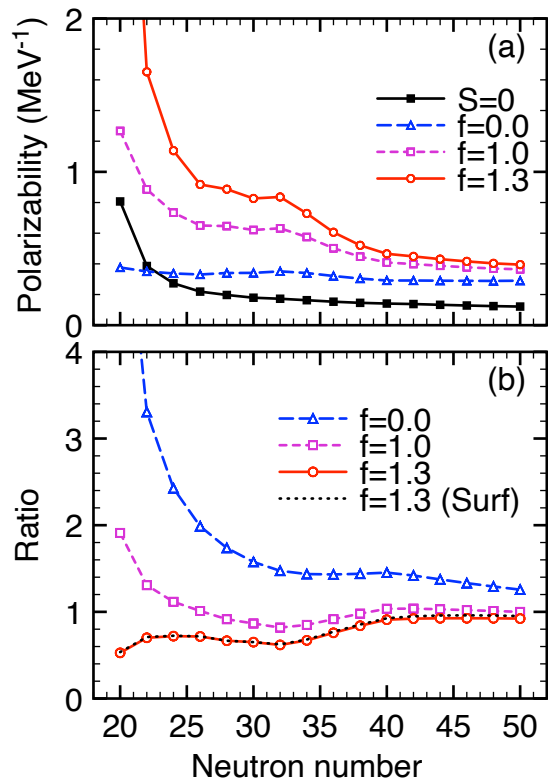


FIG. 3. (a): Polarizabilities for the pn-pair transfers with $S = 0$ and $S = 1$ for the Ca isotopes. For those with $S = 1$, the results obtained by changing f are also shown. (b): The ratio \mathcal{R}_{01} calculated by changing f . The results obtained by using the surface-type form factor are also shown for the case of $f = 1.3$ (Surf).

The method to evaluate the pn-pair collectivity, the \mathcal{R}_{01} value, from the response should not depend on details of the definitions of the pn-pair transfer operators, \hat{P}^{ad} , \hat{P}^{rm} , \hat{P}^{A} . I have examined another choice of the form factor $f(r)$ appearing in Eqs. (10) and (11) by using $f(r) = (d/dr)[1 + e^{(r-R)/a}]^{-1}$, which has a weight on the surface area of the nucleus. The results obtained by using this surface-type form factor are shown in Fig. 3(b) for the case of $f = 1.3$, in which the amplitude of the transition density is high and thus the results may be sensitive to the spatial dependence of the operator. As one can see in the figure, the \mathcal{R}_{01} value obtained is almost the same as that obtained by the volume-type form factor. I can conclude that the \mathcal{R}_{01} value does not depend on the choice of the form factor.

B. Ni and Sn isotopes

The shell effect in the $S = 1$ pn-pairing is further investigated for the Ni and Sn isotopes. The calculated pn-pair polarizabilities α_{01} , α_{10} and the ratio \mathcal{R}_{01} are shown in Fig. 4. As in the case of the Ca isotopes, the pn-pair

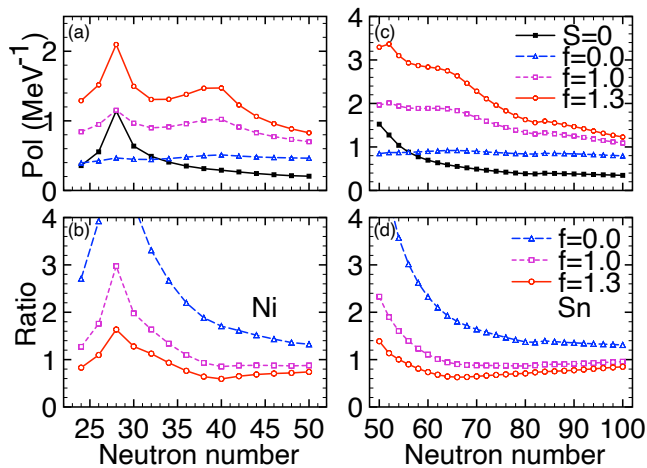


FIG. 4. As Fig. 3 but for the Ni and Sn isotopes.

polarizabilities are large at $N \approx Z$ for both $S = 0$ and $S = 1$ with inclusion of the spin-triplet pair interaction ($f > 0$). However, the $S = 1$ pn-pair polarizability α_{10} increases toward $N = 40$ in the Ni isotopes and keeps almost constant up to $N = 64$ in the Sn isotopes. This isotopic dependence is clearly seen in the ratio \mathcal{R}_{01} : one sees a minimum at $N = 40$ and 64 in the Ni and Sn isotope, respectively; the $S = 1$ pn-pair correlation is stronger than the $S = 0$ one.

The shell effect at $N = 40$ and 64 is not due to the appearance of the $S = 1$ pn-pair addition mode, as seen in the Ca isotopes, but due to that of the $S = 1$ pn-pair removal mode in low energy. Figure 5 shows the IEWS of the pn-pair addition and removal strengths. The IEWS for the $S = 1$ pn-pair removal increases toward $N = 40$ and 64 in the Ni and Sn isotopes, respectively, while the IEWSs for both the $S = 0$ pn-pair addition and removal as well as the $S = 1$ pn-pair addition decrease monotonically as stepping away from $N = Z$. It is noted that the IWSEs for the $S = 1$ pn-pair addition and removal keep almost constant as functions of the neutron number when the spin-triplet pair interaction is discarded, as expected from the calculated pair polarizability α_{10} with $f = 0$; the enhancement in the IWSE for the $S = 1$ pn-pair removal is much more significant in the calculations with $f > 1$.

A decisive role in the shell effect uniquely appearing in the $S = 1$ pn-pairing in the medium-heavy nuclei such as in the Ni and Sn isotopes is played by the occupation of the intruder proton $j_>$ orbital. Indeed, this diminishes the $S = 1$ pn-pairing in the $N \approx Z$ nuclei beyond ^{40}Ca : only either the $\pi j_> \otimes \nu j_>$ or $\pi j_< \otimes \nu j_<$ configuration is devoted to the pairing. With an increase in the neutron number from $N = Z$, the Fermi level of neutrons approaches the $j_<$ orbital. As neutrons start to occupy the $j_<$ orbital, the pair of the $\pi j_> \otimes \nu j_<$ configuration, which is exclusively in $S = 1$, appears to contribute to the pairing collectivity. In the present case, the pair of the $\pi f_{7/2} \otimes \nu f_{5/2}$ and $\pi g_{9/2} \otimes \nu g_{7/2}$ configuration gives

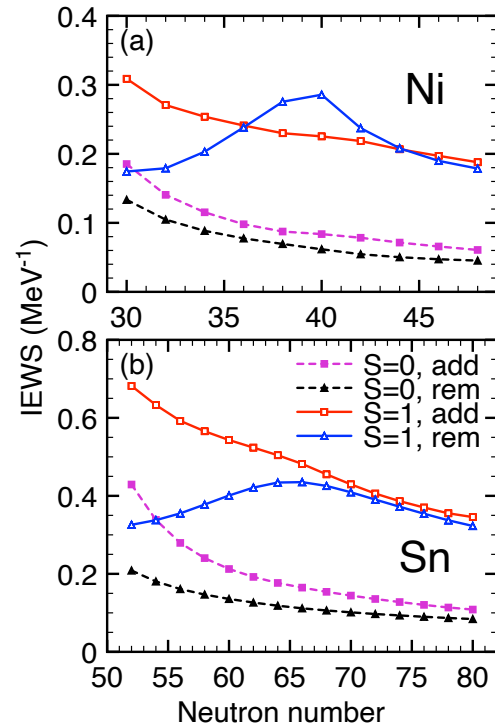


FIG. 5. IEWS of the pn-pair addition and removal strengths in (a) Ni and (b) Sn isotopes, calculated by using $f = 1.0$ for the spin-triplet pair interaction.

a significant contribution to the $S = 1$ pairing in the Ni and Sn isotopes, respectively.

IV. SUMMARY

Proton-neutron (pn) pair correlations have been investigated in the Ca, Ni, and Sn isotopes as examples of medium-heavy nuclei. The collectivity was quantified by introducing the polarizability for the response to pn-pair transfers. The polarizabilities were evaluated in the framework of the nuclear energy-density functional method.

The spin-singlet pn-pair correlation is the strongest at $N = Z$ and decreases monotonically as the neutron number increases. In contrast, the spin-triplet pn-pair correlation is shown to depend non-monotonically on the neutron number and can be enhanced in cases where the pn-pair removal modes involving the $\pi j_> \otimes \nu j_<$ configuration occur at low energy. Therefore, the relative strength of spin-triplet and spin-singlet pn-pair correlations becomes large in the neutron-rich isotopes when neutrons occupy the $j_<$ orbital.

ACKNOWLEDGMENTS

The author acknowledges the invaluable contributions of members of the PHANES Collaboration, particularly M. Dozono, M. Matsuo, S. Ota, and S. Shimoura, for their insightful discussions. This work was supported by JSPS KAKENHI (Grant No. JP23H05434), and JST

ERATO (Grant No. JPMJER2304). The numerical calculations were performed on the computing facilities at the Yukawa Institute for Theoretical Physics, Kyoto University, and at the Research Center for Nuclear Physics, Osaka University. This work also used computational resources of SQUID provided by the D3 Center, Osaka University through the HPCI System Research Project (Project ID: hp230085).

-
- [1] J. Bardeen, L. N. Cooper, and J. R. Schrieffer, Microscopic theory of superconductivity, *Phys. Rev.* **106**, 162 (1957).
- [2] A. Bohr and B. Mottelson, *Nuclear Structure: Volume II, Nuclear Deformations* (Benjamin, 1969).
- [3] P. Ring and P. Schuck, *The nuclear many-body problem* (Springer-Verlag, New York, 1980).
- [4] G. F. Bertsch, Nuclear pairing: Basic phenomena revisited, in *Fifty Years of Nuclear BCS*, pp. 26–39.
- [5] S. Yoshida, Note on the two-nucleon stripping reaction, *Nucl. Phys.* **33**, 685 (1962).
- [6] A. Goswami and L. S. Kisslinger, Particle correlation arising from isospin pairing in light nuclei, *Phys. Rev.* **140**, B26 (1965).
- [7] A. L. Goodman, Proton-neutron pairing in $Z = N$ nuclei with $A = 76$ –96, *Phys. Rev. C* **60**, 014311 (1999).
- [8] A. Gezerlis, G. F. Bertsch, and Y. L. Luo, Mixed-spin pairing condensates in heavy nuclei, *Phys. Rev. Lett.* **106**, 252502 (2011), [arXiv:1103.5793 \[nucl-th\]](#).
- [9] A. Poves and G. Martinez-Pinedo, Pairing and the structure of the pf -shell $N \sim Z$ nuclei, *Phys. Lett. B* **430**, 203 (1998).
- [10] G. F. Bertsch and Y. Luo, Spin-triplet pairing in large nuclei, *Phys. Rev. C* **81**, 064320 (2010), [arXiv:0912.2533 \[nucl-th\]](#).
- [11] T. Alm, G. Röpke, and M. Schmidt, Neutron-proton pairing in symmetric nuclear matter, *Z. Phys. A* **337**, 355 (1990).
- [12] B. Vonderfecht, C. Gearhart, W. Dickhoff, A. Polls, and A. Ramos, Bound pair states in nuclear matter, *Phys. Lett. B* **253**, 1 (1991).
- [13] M. Baldo, I. Bombaci, and U. Lombardo, Nuclear matter superfluidity in the S–D channel, *Phys. Lett. B* **283**, 8 (1992).
- [14] T. Takatsuka and R. Tamagaki, Superfluidity in Neutron Star Matter and Symmetric Nuclear Matter, *Prog. Theor. Phys. Suppl.* **112**, 27 (1993).
- [15] S. Frauendorf and A. O. Macchiavelli, Overview of neutron–proton pairing, *Prog. Part. Nucl. Phys.* **78**, 24 (2014), [arXiv:1405.1652 \[nucl-th\]](#).
- [16] L. Capelli, G. Colo, and J. Li, Dielectric theorem within the Hartree-Fock-Bogoliubov framework, *Phys. Rev. C* **79**, 054329 (2009).
- [17] A. Tamii, I. Poltoratska, P. von Neumann-Cosel, Y. Fujita, T. Adachi, C. A. Bertulani, J. Carter, M. Dozono, H. Fujita, K. Fujita, K. Hatanaka, D. Ishikawa, M. Itoh, T. Kawabata, Y. Kalmykov, A. M. Krumbholz, E. Litvinova, H. Matsubara, K. Nakanishi, R. Neveling, H. Okamura, H. J. Ong, B. Özel-Tashenov, V. Y. Ponomarev, A. Richter, B. Rubio, H. Sakaguchi, Y. Sakemi, Y. Sasamoto, Y. Shimbara, Y. Shimizu, F. D. Smit, T. Suzuki, Y. Tameshige, J. Wambach, R. Yamada, M. Yosoi, and J. Zenihiro, Complete electric dipole response and the neutron skin in ^{208}Pb , *Phys. Rev. Lett.* **107**, 062502 (2011).
- [18] J. Piekarewicz, B. K. Agrawal, G. Colo, W. Nazarewicz, N. Paar, P. G. Reinhard, X. Roca-Maza, and D. Vretenar, Electric dipole polarizability and the neutron skin, *Phys. Rev. C* **85**, 041302 (2012), [arXiv:1201.3807 \[nucl-th\]](#).
- [19] X. Roca-Maza and N. Paar, Nuclear equation of state from ground and collective excited state properties of nuclei, *Prog. Part. Nucl. Phys.* **101**, 96 (2018), [arXiv:1804.06256 \[nucl-th\]](#).
- [20] K. Takahashi, Y. Matsuda, and M. Matsuo, Higgs response and pair condensation energy in superfluid nuclei, *PTEP* **2023**, 083D01 (2023), [arXiv:2302.14214 \[nucl-th\]](#).
- [21] K. Yoshida, Isovector giant monopole and quadrupole resonances in a Skyrme energy density functional approach with axial symmetry, *Phys. Rev. C* **104**, 044309 (2021), [arXiv:2107.00867 \[nucl-th\]](#).
- [22] P. Frobrich, Enhancement of deuteron transfer reactions by neutron-proton pairing correlations, *Phys. Lett. B* **37**, 338 (1971).
- [23] P. V. Isacker, D. D. Warner, and A. Frank, Deuteron Transfer in $N = Z$ Nuclei, *Phys. Rev. Lett.* **94**, 162502 (2005).
- [24] J. Lay, Y. Ayyad, and A. Macchiavelli, Neutron-proton pair transfer reactions and corresponding weisskopf-type units, *Phys. Lett. B* **824**, 136789 (2022).
- [25] K. Yoshida, Spin–isospin response of deformed neutron-rich nuclei in a self-consistent Skyrme energy-density-functional approach, *PTEP* **2013**, 113D02 (2013), [Erratum: PTEP 2021, 019201 (2021)], [arXiv:1308.0424 \[nucl-th\]](#).
- [26] J. Dobaczewski, H. Flocard, and J. Treiner, Hartree-Fock-Bogolyubov descriptions of nuclei near the neutrino dripline, *Nucl. Phys. A* **422**, 103 (1984).
- [27] H. Kasuya and K. Yoshida, Hartree-Fock-Bogoliubov theory for odd-mass nuclei with a time-odd constraint and application to deformed halo nuclei, *PTEP* **2021**, 013D01 (2021), [arXiv:2005.03276 \[nucl-th\]](#).
- [28] T. Nakatsukasa, K. Matsuyanagi, M. Matsuo, and K. Yabana, Time-dependent density-functional description of nuclear dynamics, *Rev. Mod. Phys.* **88**, 045004 (2016), [arXiv:1606.04717 \[nucl-th\]](#).
- [29] K. Yoshida and N. Van Giai, Deformed quasiparticle-random-phase approximation for neutron-rich nuclei using the Skyrme energy density functional, *Phys. Rev. C* **78**, 064316 (2008), [arXiv:0809.0169 \[nucl-th\]](#).
- [30] S. Ebata, T. Nakatsukasa, T. Inakura, K. Yoshida, Y. Hashimoto, and K. Yabana, Canonical-basis time-dependent Hartree-Fock-Bogoliubov theory and linear

- response calculations, *Phys. Rev. C* **82**, 034306 (2010), [arXiv:1007.0785 \[nucl-th\]](#).
- [31] G. Scamps and D. Lacroix, Systematic study of isovector and isoscalar giant quadrupole resonances in normal and superfluid deformed nuclei, *Phys. Rev. C* **89**, 034314 (2014), [arXiv:1401.5211 \[nucl-th\]](#).
- [32] N. van Giai and H. Sagawa, Spin-isospin and pairing properties of modified Skyrme interactions, *Phys. Lett. B* **106**, 379 (1981).
- [33] M. Yamagami, Y. R. Shimizu, and T. Nakatsukasa, Optimal pair density functional for description of nuclei with large neutron excess, *Phys. Rev. C* **80**, 064301 (2009), [arXiv:0812.3197 \[nucl-th\]](#).
- [34] Y. Fujita, H. Fujita, T. Adachi, C. L. Bai, A. Algora, G. P. A. Berg, P. von Brentano, G. Colò, M. Csatlós, J. M. Deaven, E. Estevez-Aguado, C. Fransen, D. De Frenne, K. Fujita, E. Ganioglu, C. J. Guess, J. Gulyás, K. Hatanaka, K. Hirota, M. Honma, D. Ishikawa, E. Jacobs, A. Krasznahorkay, H. Matsubara, K. Matsuyanagi, R. Meharchand, F. Molina, K. Muto, K. Nakanishi, A. Negret, H. Okamura, H. J. Ong, T. Otsuka, N. Pietralla, G. Perdikakis, L. Popescu, B. Rubio, H. Sagawa, P. Sarriguren, C. Scholl, Y. Shimbara, Y. Shimizu, G. Susoy, T. Suzuki, Y. Tameshige, A. Tamii, J. H. Thies, M. Uchida, T. Wakasa, M. Yosoi, R. G. T. Zegers, K. O. Zell, and J. Zenihiro, Observation of Low- and High-Energy Gamow-Teller Phonon Excitations in Nuclei, *Phys. Rev. Lett.* **112**, 112502 (2014).
- [35] Y. Fujita, H. Fujita, T. Adachi, G. Susoy, A. Algora, C. L. Bai, G. Colò, M. Csatlós, J. M. Deaven, E. Estevez-Aguado, C. J. Guess, J. Gulyás, K. Hatanaka, K. Hirota, M. Honma, D. Ishikawa, A. Krasznahorkay, H. Matsubara, R. Meharchand, F. Molina, H. Nakada, H. Okamura, H. J. Ong, T. Otsuka, G. Perdikakis, B. Rubio, H. Sagawa, P. Sarriguren, C. Scholl, Y. Shimbara, E. J. Stephenson, T. Suzuki, A. Tamii, J. H. Thies, K. Yoshida, R. G. T. Zegers, and J. Zenihiro, High-resolution study of Gamow-Teller excitations in the $^{42}\text{Ca}(^3\text{He}, t)^{42}\text{Sc}$ reaction and the observation of a “low-energy super-Gamow-Teller state”, *Phys. Rev. C* **91**, 064316 (2015).
- [36] H. Fujita, Y. Fujita, Y. Utsuno, K. Yoshida, T. Adachi, A. Algora, M. Csatlós, J. M. Deaven, E. Estevez-Aguado, C. J. Guess, J. Gulyás, K. Hatanaka, K. Hirota, R. Hutton, D. Ishikawa, A. Krasznahorkay, H. Matsubara, F. Molina, H. Okamura, H. J. Ong, G. Perdikakis, B. Rubio, C. Scholl, Y. Shimbara, G. Süsoy, T. Suzuki, A. Tamii, J. H. Thies, R. G. T. Zegers, and J. Zenihiro, Experimental study of Gamow-Teller transitions via the high-energy-resolution $^{18}\text{O}(^3\text{He}, t)^{18}\text{F}$ reaction: Identification of the low-energy “super” -Gamow-Teller state, *Phys. Rev. C* **100**, 034618 (2019).
- [37] K. Yoshida, Suddenly shortened half-lives beyond ^{78}Ni : $N = 50$ magic number and high-energy non-unique first-forbidden transitions, *Phys. Rev. C* **100**, 024316 (2019), [arXiv:1903.03310 \[nucl-th\]](#).
- [38] K. Yoshida, Proton-neutron pairing vibrations in $N = Z$ nuclei: Precursory soft mode of isoscalar pairing condensation, *Phys. Rev. C* **90**, 031303 (2014), [arXiv:1409.4884 \[nucl-th\]](#).
- [39] R. Broglia and D. Bes, High-lying pairing resonances, *Phys. Lett. B* **69**, 129 (1977).
- [40] F. Cappuzzello, D. Carbone, M. Cavallaro, M. Bondi, C. Agodi, F. Azaiez, A. Bonaccorso, A. Cunsolo, L. Fortunato, A. Foti, S. Franchoo, E. Khan, R. Linares, J. Lubian, J. A. Scarpaci, and A. Vitturi, Signatures of the Giant Pairing Vibration in the ^{14}C and ^{15}C atomic nuclei, *Nat. Comm.* **6**, 6743 (2015).
- [41] M. Assié, C. H. Dasso, R. J. Liotta, A. O. Macchiavelli, and A. Vitturi, The giant pairing vibration in heavy nuclei, *Eur. Phys. J. A* **55**, 245 (2019).
- [42] M. Cavallaro, F. Cappuzzello, D. Carbone, and C. Agodi, Giant pairing vibrations in light nuclei, *Eur. Phys. J. A* **55**, 244 (2019).